An Experimental and Computational Study on the Rate Constant of Electrochemically Generated *N*-Acetyl-*p*-Quinoneimine with Dimethylamine

Hadi Shafiei[1], Mohammad Haqgu[2], Davood Nematollahi[3,*], Mohammad R. Gholami[4]

[1] Science and Research Branch, Islamic Azad University, P.O. Box 14515-775, Tehran, Iran
[2] Islamic Azad University, Branch of Hamadan, Hamadan, Iran
[3] Faculty of Chemistry, Bu-Ali-Sina University, Hamadan 65174, Iran
[4] Department of Chemistry, Sharif University of Technology, Tehran, lran
[*]E-mail: nemat@basu.ac.ir

Electrochemical oxidation of acetaminophen (*N*–acetyl–*p*–aminophenol) (**1**) has been studied in the presence of dimethylamine (**2**) as a nucleophile in aqueous solution, by means of cyclic voltammetry and controlled-potential coulometry. The results indicate the participation of electrochemically generated *N*-acetyl-*p*-quinoneimine (**1a**) in Michael reaction with dimethylamine (**2**). Based on *ECE* mechanism, the observed homogeneous rate constant (k_{obs}) of the above mentioned reaction is estimated by comparing the experimental cyclic voltammograms with the digital simulated results. Further more; kinetics and mechanism of the reaction were studied with ab initio calculation, Monte Carlo and QM/MM simulations in gas phase and aqueous phase. Geometrical parameters and charge calculations show that these reactions proceed through the 1,4-Michael addition mechanism and first step of mentioned reaction is rate determining. Solvent effects on these reactions were studied by inserting water molecules in reaction media, Onsager model, Monte Carlo and QM/MM simulations. Activation parameters indicate the expected variation in activation energy and reaction coordinate in aqueous phase in comparison to the gas phase. The free energy perturbation calculation from Monte Carlo simulation yielded the profiles along a reaction coordinate. Free energies of activation have been computed to be in close agreement with experimental values.

1. INTRODUCTION

Acetaminophen (**1**) is one of the most widely used over-the-counter drugs with analgesic and antipyretic properties. Although regarded to be safe at therapeutic doses, acetaminophen is known to

cause acute hepatic centrilobular necrosis in humans when consumed in large doses [1,2]. The mechanism of acetaminophen-induced toxicity has come under extensive study and circumstantial evidence for the involvement of the cytochrome P460 mixed function oxidize in the formation of an electrophilic reactive intermediate is strong [3-9]. Nowadays, it is generally accepted that acetaminophen is bioactivated in the liver by cytochromes P450 by two pathways to form a reactive and toxic intermediate, *N*-acetyl-*p*-quinoneimine (**1a**) [10-14] and a nontoxic catechol metabolite, 3'-hydroxyacetaminophen [15-17]. With therapeutic doses, a large proportion of the acetaminophen is excreted as the glucuronide and sulfate conjugates and most of the *N*-acetyl-*p*-quinoneimine formed reacts with glutathione to ultimately become water soluble, nontoxic metabolites which are excreted [18]. When a larger dose is administered, the level of glutathione is depleted and the quinoneimine reacts with cell macromolecules leading to cell damage or death [19]. Also, electrochemical methods, especially the voltammetric and amperometric ones give the opportunity to study the oxidation mechanisms, the redox metabolites and their detection from pharmaceuticals and body fluids [20-31]. The cyclic voltammetric study concerning the electrochemical oxidation of acetaminophen (**1**) was described in the works of Kissinger et al. [20,21]. The first reaction is an electrochemical oxidation by a two-electron, two-proton process, and the result is *N*-acetyl-*p*-quinoneimine (**1a**), and the final product is *p*-benzoquinone (**1d**) (Scheme 1).
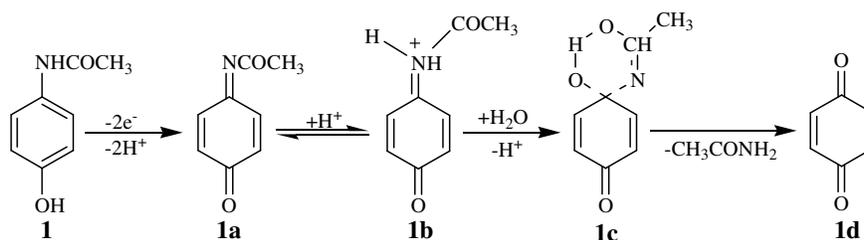
Scheme 1.

Since electrochemical oxidation very often parallels the cytochrome P450 catalyzed oxidation in liver microsomes, studying the anodic oxidation of acetaminophen in the presence of nucleophiles was of interest. Therefore, with the aim of investigating of the reactivity of intermediate *N*-acetyl-*p*-quinoneimine (**1a**) toward amines, as well as estimation of observed chemical rate constant of this reaction, we investigated the electrochemical oxidation of acetaminophen in aqueous solutions in the presence of dimethylamine (**2**) as a model for amine important compounds such as drugs, amino acids, peptides and proteins. Also, we present the theoretical calculations of the observed homogeneous rate constant (k_{obs}) of Michael reaction of *N*-acetyl-*p*-quinoneimine (**1a**) with dimethylamine (**2**) which is also compared with the experimental value. In addition, in this work we have used the ab initio molecular orbital calculations, QM/MM and Monte Carlo simulation to study the solvent effect on the reaction of *N*-acetyl-*p*-quinoneimine (**1a**) and dimethylamine (**2**).

2. EXPERIMENTAL PART

2.1. Apparatus

Cyclic voltammetry and controlled-potential coulometry were performed using a Behpajoh model BHP-2062 potentiostat/galvanostat. The working electrode used in the voltammetry experiments was a glassy carbon disc (1.8 mm diameter) and platinum wire was used as the counter electrode. The working electrode potentials were measured versus standard calomel electrode (SCE) (all electrodes from Azar Electrode).

2.2. Reagents

All chemicals (acetaminophen and dimethylamine) were reagent-grade materials, from Aldrich. Sodium carbonate was of pro-analysis grade from E. Merck. These chemicals were used without further purification. The homogeneous rate constants were estimated by analyzing the cyclic voltammetric responses using the DigiElch simulation software [32].

2.3. Computational detail

The structures corresponding to the reactant, intermediate and TS were optimized, using the Gaussian 98 computational package [33] with the ab initio method at the RHF level in the 6-31G* basis set [34]. The synchronous transit-guided quasi-Newton (STQN) method as implemented by Schlegel et al. [35] was used to locate the TSs. Vibrational frequencies for the points along the reactions paths were determined to provide an estimation of the zero point vibrational energies (ZPVEs). These calculations verified the nature of the stationary points as minima with the real frequencies and the TSs with only one imaginary frequency.

The TS has not been located at B3LYP/6-31G* DFT methods despite an extensive search.

To investigate solvent effects on ab initio calculations, reactants and TS were optimized in presence of a few water molecules. Also calculations of reaction field were carried out with the Onsager model. In the field model solvent is represented by continuous dielectric which characterized by a given dielectric constant (ε). The solute is assumed to be embedded into a special cavity with radii a_0.

QM/MM calculations in solution were carried out using the DYNAMO program [36]. The reacting system was treated by AM1, placed in a cavity deleted from a 24.66 Å cubic box of 500 water molecules described by non-rigid TIP3P empirical potentials [37]. A solvent boundary potential was employed to prevent evaporation of water molecules from the surface of the box during the optimizations. The nonbonding interactions were calculated using an atom-based switching function with inner and outer cutoffs of 8.0 and 12.0 Å. Finally the full system was optimized up to a gradient tolerance of 0.1 kJ/mol.

The reaction coordinate was defined as N_2-C_2 bond lengths (Scheme 5). For Monte Carlo simulation the structures that located in minimum energy reaction path (MERP) were determined at QM/MM AM1/TIP3P levels at fixed values of Rc.

Lennard-Jones parameters for solute were taken from all-atom force field [38]. The TIP3P model was adapted for water. The partial charges for the solute atoms were those from the RHF/6-31G* CHELPG calculations. The Monte Carlo simulations were executed in the NVT ensemble at 298 ^{o}K with metropolis sampling and periodic boundary conditions. The cubic cell contained 500 water molecules plus the reacting system with dimensions of 25x25x25 Å^3. Free energy perturbation theory with Monte Carlo simulation was then used to obtain the changes in free energies of solvation along the reaction path. These calculations were performed in a program that was written in FORTRAN language [39]. Activation energy E_a and rate constant k were computed at 298 ^{o}K using the equations (1) and (2), respectively.

$$E_a = \Delta H^{\#}(T) + RT \qquad\qquad (1)$$

$$k = k_B T/h \, \exp(-\Delta G^{\#}/RT) \qquad\qquad (2)$$
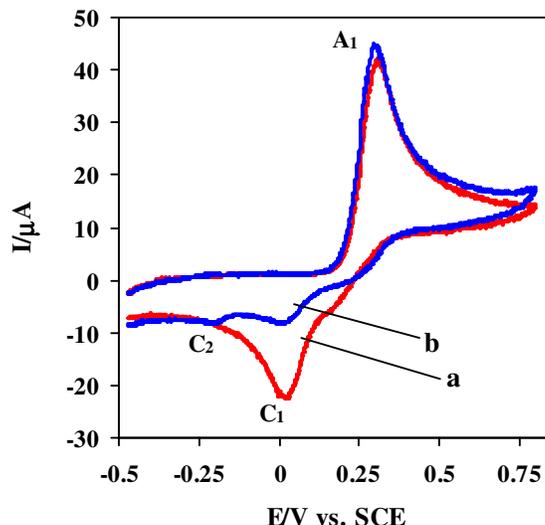
Figure 1. Cyclic voltammograms of acetaminophen (**1**) (2 mM): (a) in the absence, (b) in the presence of 20 mM dimethylamine, at glassy carbon electrode (1.8 mm diameter) in aqueous solution containing 0.5 M carbonate buffer (pH 10.0). Scan rate: 250 mV/s; t =25±1°C.

3. RESULTS AND DISCUSSION

3.1. Electrochemical studies

The electrochemical study of 2 mM solution of acetaminophen (**1**) in an aqueous solution containing 0.5 M carbonate buffer (pH 10.0), at a bare glassy carbon electrode has been performed

using cyclic voltammetry (Fig. 1, curve a). The voltammogram shows one anodic (A_1) and corresponding cathodic peak (C_1), at 0.35 V and about 0.0 V versus standard calomel electrode (SCE), respectively, which correspond to the transformation of acetaminophen (**1**) to *N*-acetyl-*p*-quinoneimine (**1a**) and vice-versa within a quasi-reversible two-electron process (Scheme 2, Eq. 1) [20,21].

Because of the reactions mentioned in Scheme 1, the peak current ratio (I_p^{C1}/I_p^{A1}) is less than unity, decreases with decreasing pH and increases with increasing scan rate (Fig. 2).

The oxidation of acetaminophen (**1**) in the presence of dimethylamine (**2**) as a nucleophile was studied in some detail. Figure 1, (curve b) shows the cyclic voltammogram obtained for a 2 mM solution of **1** in the presence of 20 mM dimethylamine (**2**). In this case, the cathodic counterpart of the anodic peak A_1 decreases and voltammogram exhibits two cathodic peaks (C_1 and C_0).
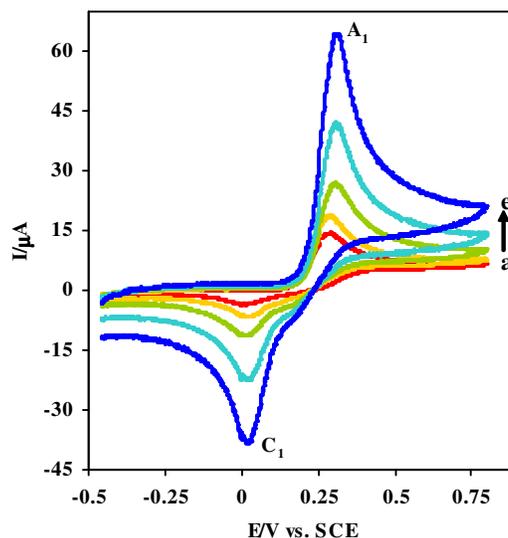

Figure 2. Typical cyclic voltammograms of 2 mM acetaminophen (**1**) at glassy carbon electrode (1.8 mm diameter), in aqueous solution containing carbonate buffer (pH 10.0, c = 0.5 M). Scan rates from (a) to (e) are: 25, 50, 100, 250 and 500 mVs^{-1}, respectively. t =25±1°C.

Also, it is seen that, proportionally to the augmentation of the potential sweep the height of C_1 increases and the height of C_0 decreases (Fig. 3). In other words, the peak current ratio (I_p^{C1}/I_p^{A1}) vs. scan rate for a mixture of acetaminophen (**1**) and dimethylamine (**2**) increases with increasing scan rate, confirm the reactivity of **1a** towards **2** A similar situations is observed when the dimethylamine (**2**) to **1** concentration ratio is decreased. Besides the current function for peak A_1 ($I_p^{A1}/v^{1/2}$) decreases with increasing scan rate. These observations allow us to propose a mechanistic pathway for the cyclic voltammetric behavior of acetaminophen (**1**) in the presence of dimethylamine (**2**), depicted in Scheme 2.
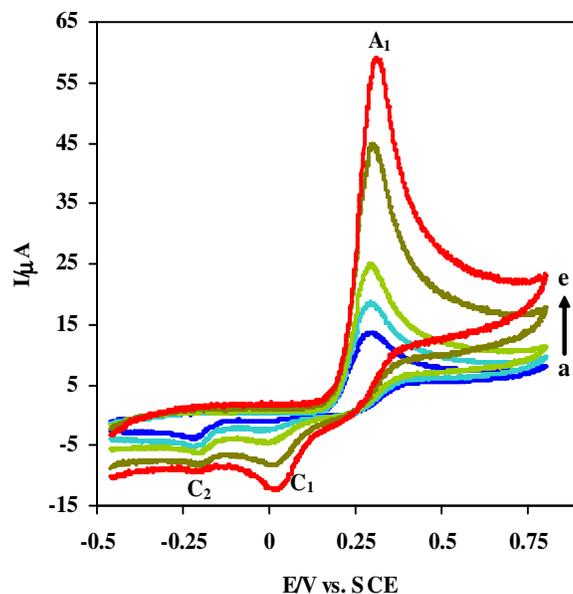
Figure 3. Typical cyclic voltammograms of 2 mM acetaminophen in the presence of 20 mM dimethylamine at glassy carbon electrode, in aqueous solution containing carbonate buffer (pH 10.0 and c = 0.5 M). Scan rates from (a) to (e) are: 25, 50, 100, 250 and 500 mVs^{-1}, respectively. t =25±1°C.
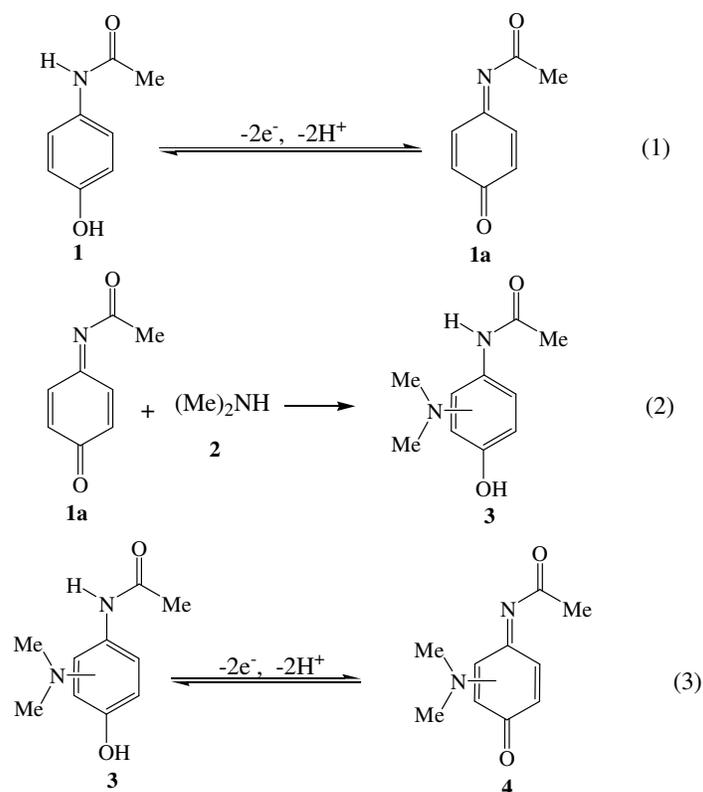

Scheme 2.

According to our results, it seems that the 1,4-Michael addition reaction of **2** to *N*-acetyl-*p*-quinoneimine (**1a**) leads to intermediate **3**. The oxidation of this compound (**3**) is easier than the oxidation of parent starting molecule (**1**) by virtue of the presence of electron-donating group. The reaction product (**4**) can also be attacked by **2**. However, this reaction was not observed during the voltammetric experiments because of the low reactivity of the product (**4**) toward Michael addition, arising from the presence of an electron-donating group on the p-quinoneimine ring.

3.2. Digital simulation

The scheme for the electrochemical oxidation of acetaminophen (**1**) in the presence of dimethylamine (**2**) was proposed and tested by digital simulation. The transfer coefficient (α) was assumed to be 0.5 and the formal potential was obtained experimentally as the midpoint potential between the anodic and cathodic peaks (E_{mid}). The heterogeneous rate constant (0.002 cm s^{-1}) for oxidation of acetaminophen (**1**) was estimated by use of an experimental working curve [29]. All parameters were kept constant through out the fitting of the digitally simulated voltammogram to the experimental data. The parameter k_{obs} was allowed to change through the fitting processes. Further refinement was accomplished by holding the best-fit parameters and varying (slightly) of D (1.0 $\pm$ 0.3x10^{-5} cm^2 s^{-1}) throughout the fitting process. The observed homogeneous rate constant (k_{obs}) of the reaction of *N*-acetyl-*p*-quinoneimine (**1a**) with dimethylamine (**2**) was estimated by comparison of the simulation results with experimental cyclic voltammograms. The simulated cyclic voltammograms show good agreement with those obtained experimentally. (Fig. 4), confirm the mechanism *ECE* in electrochemical oxidation of acetaminophen (**1**) in the presence of dimethylamine (**2**). The calculated observed homogeneous rate constant is 0.078 ($RSD_{n=4}$ = 7.3 %).
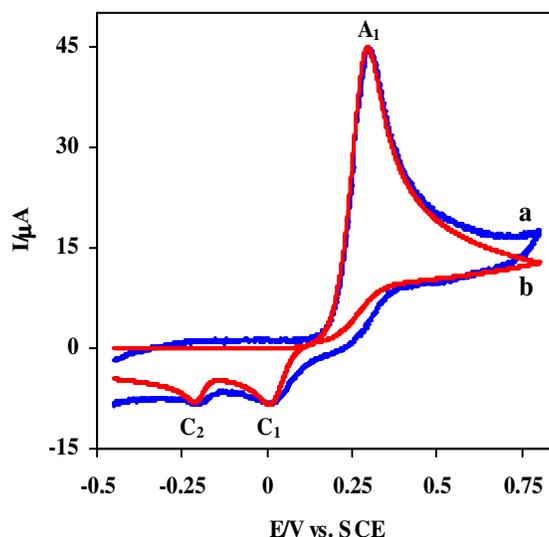
Figure 4. Experimental (curve a blue color) and simulated (curve b red color) cyclic voltammograms of 2 mM acetaminophen (**1**), in the presence of 20 mM dimethylamine (**2**) at glassy carbon electrode, in carbonate buffer solution (pH 10.0, c = 0.5 M). Scan rate: 250 mV s^{-1}. Simulation performed base on *ECE* electrochemical mechanism.

3.3. Reaction mechanism and reaction pathway

The electro-oxidation of acetaminophen (**1**) in the presence of dimethylamine (**2**) is considered to involve the Michael acceptor *N*-acetyl-*p*-quinoneimine (**1a**) as an intermediate that could be attacked at positions A or B to yield **4a** and **4b** respectively (Scheme 3).
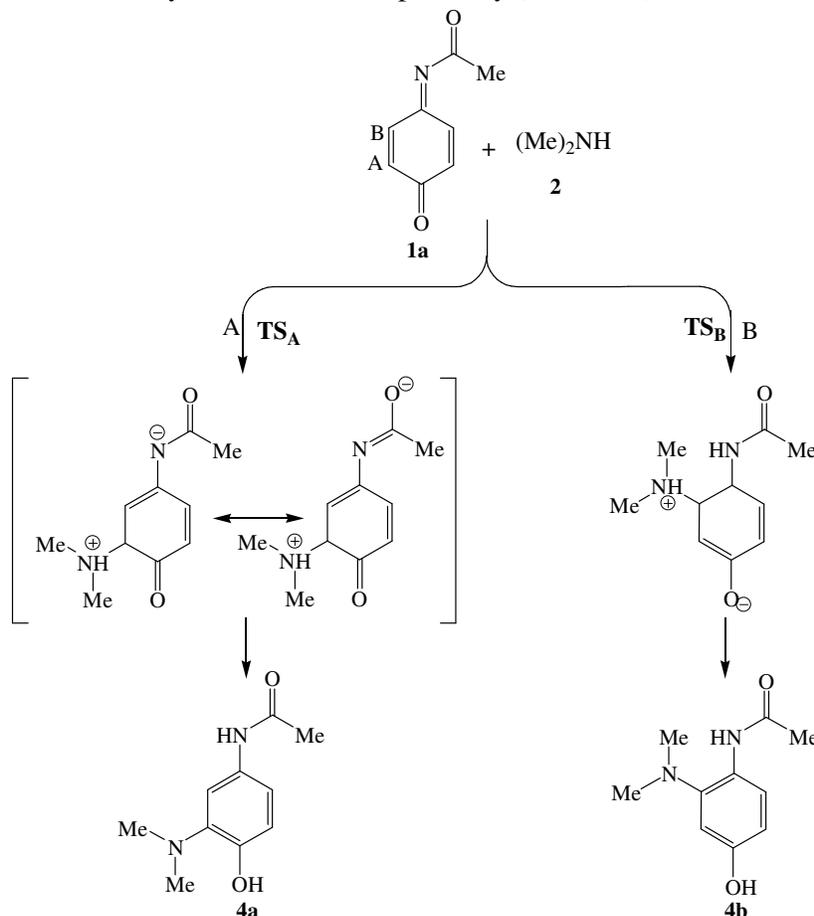
Scheme 3.

The profile of energy changes of the two pathways at QM/MM AM1/TIP3P levels of theory are shown in Fig 5. It is observed that the process barrier of nucleophilic attack for pathway of B is higher than pathway of A. Therefore according to the obtained results and the previous reports [40,41] reaction between **1a** and **2** happens in pathway A. Figure 5 shows that the AM1/TIP3P barrier to reaction, which is about 13.5 kcal/mol. Since, if the second step of the proposed mechanisms is the rate determination step, the both *N*-(3-dimethylamino-4-hydroxyphenyl)-acetamide (**4a**) and *N*-(2-dimethylamino-4-hydrox yphenyl)-acetamide (**4b**) products generation is possible. However previous reports [40,41] show that only **4a** is generated. This observation indicated the rate determination step is the first step. Since the pathway A had lower energy it was chosen for further study.
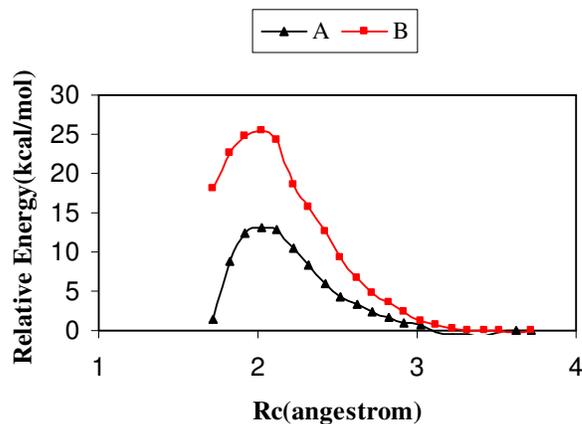
Figure 5. The profiles of energy changes pathway A and B for **1a** and **2** reaction at QM/MM AM1/TIP3P levels of theory.

3.4. Gas phase results

In order to study kinetics and mechanism of the reactions, structure corresponding to reactants, transition states and products were optimized in RHF/6-31G* level of theory. Scheme 4 shows the optimized structures of reactants, TS and intermediate for path A in Scheme 3. Their selected geometrical parameters are shown in Table 1.

From Table 1, it is obvious that C_1-C_2, C_6-N_{11} and $C_{12}-O_{13}$ bonds increase and C_1-C_6 and $N_{11}-C_{12}$ bonds decrease in TS respect to reactants. This coincides with electron movement shown in Scheme 3, path A.
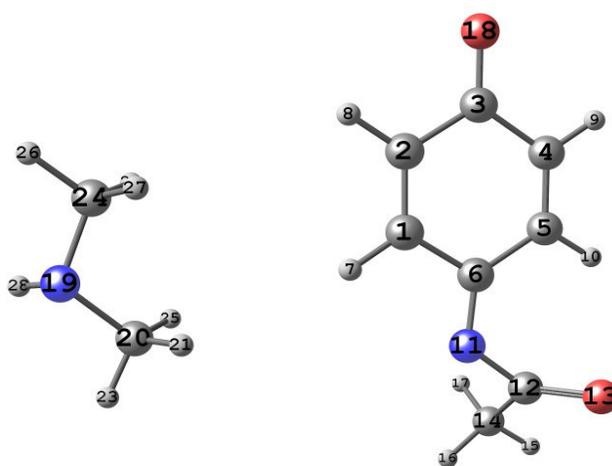
Reactants
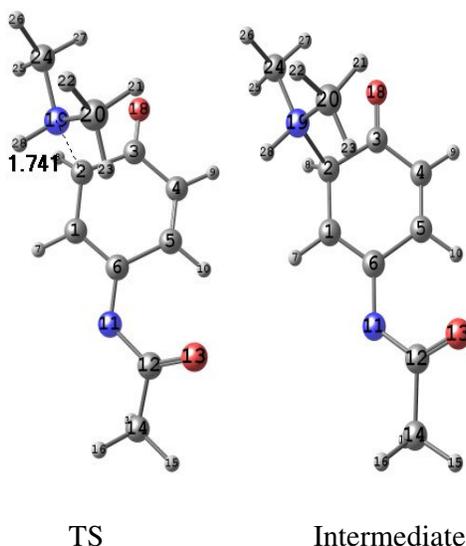
TS   Intermediate

Scheme 4. Optimized structures of reactants, TS and intermediate of Scheme 3, path A

Table 1. Selected geometrical parameters for reactants TS and products of Scheme 3, path A in RHF/6-31G* levels of theory (distances in angstrom and angles in degree)

	Reactants	TS	Intermediate
R(1-2)	1.324	1.426	1.472
R(1-6)	1.480	1.393	1.366
R(2-3)	1.484	1.523	1.534
R(3-4)	1.487	1.467	1.457
R(3-18)	1.195	1.198	1.201
R(4-5)	1.325	1.328	1.332
R(4-9)	1.074	1.075	1.075
R(5-6)	1.483	1.507	1.505
R(6-11)	1.262	1.308	1.330
R(11-12)	1.402	1.363	1.347
R(12-13)	1.191	1.211	1.219
R(12-14)	1.507	1.514	1.517
R(19-20)	1.447	1.474	1.488
R(19-24)	1.447	1.475	1.486
R(19-28)	1.001	1.005	1.006

3.5. Solvent effect

3.5.1. Onsager model

In order to investigate the solvent effects using Onsager model, the volume calculations were used to determine the optimized structures radii in the gas phase. The calculated radius was then applied in optimization of gas phase structures in aqueous phase. The optimizations were performed in RHF/6-31G* level of theory and the frequency calculations were performed at this level. The E_a, free

energy of activation ($\Delta G^{\#}$) and the rate constants (k) for the reaction were calculated from thermodynamic quantities. The results are summarized in Table 2. According to this Table, the activation energy of reaction (path A, in Scheme 3) decreases by solvent effects as expected. However, this model does not correctly predict the free energy of activation ($\Delta G^{\#}$) or the rate constant (k) correctly. This discrepancy is due to the fact that the use of the nonspecific interactions, implemented in this model, is not sufficient and the specific solute-solvent interactions, such as hydrogen bonding, must be considered.

Table 2. E_a, $\Delta G^{\#}$ and k values for path A, Scheme 3

	E_a/(kcal.mol^{-1})	$\Delta G^{\#}$/(kcal.mol^{-1})	k/(l.mol^{-1}.s^{-1})
Gas phase	36.87	49.59	2.59E-24
Onsager	29.46	41.78	1.39E-18
Monte Carlo	---	22.89	1.00E-4
Experiment	---	21.00*	0.01

*Obtained from Eq. 2.

3.5.2. QM/MM simulation

The key geometrical parameter TS from QM/MM AM1/TIP3P calculation are given in Scheme 5. Obtained results reveal that the reaction coordinate at TS is 0.2 Å longer upon transfer to solution. The result from Onsager (RHF/6-31G*) method confirms this result.

a) b)
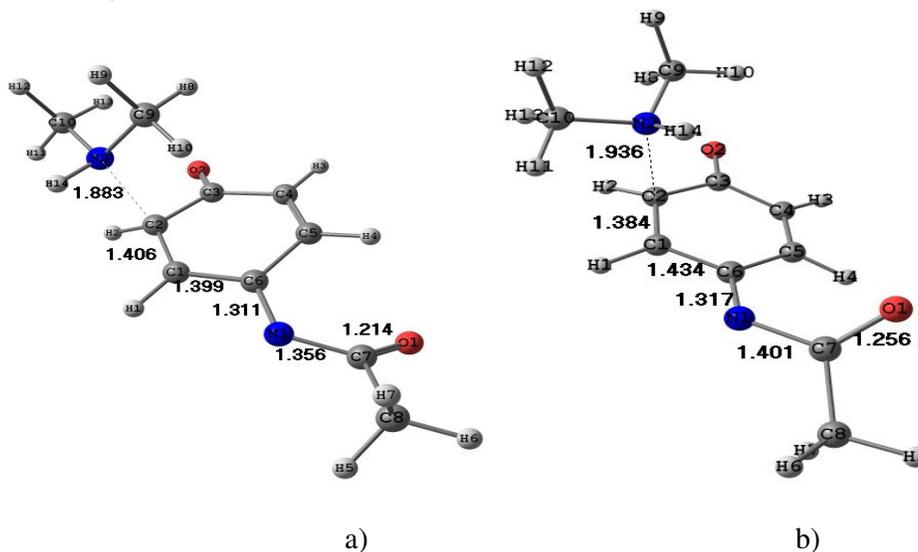
Scheme 5. Optimized geometry of TS from a) Onsager (RHF/6-31G*) method, b) QM/MM AM1/TIP3P calculation

Charge distribution in the reactants and TS were calculated by the RHF/6-31G* CHELPG analysis. This analysis shows a large change in charges of O_1, N_1, C_1, and N_2 atoms (Scheme 5). Charges on N_2 atom are increased to positive values in TS with respect to reactants, while Charges on O_1, N_1 and C_1 atoms are increased to negative values in the reaction (Table 3). In another words negative charge is translated from N_2 atom to O_1, N_1 and C_1 atoms.

Table 3. Electric charge variations in TS with respect to reactants in water media.

| Atom	QM/MM	
	Reactant	TS
O_1	-0.612	-0.674
C_7	0.984	0.978
N_1	-0.780	-0.864
C_6	0.725	0.800
C_1	-0.257	-0.776
C_2	-0.204	0.116
N_2	-0.759	0.167
H_{14}	0.379	0.162

3.5.3. Monte Carlo method

Monte Carlo simulation was applied to study the solvent effects on the reaction. The structures located in MERP were determined by QM/MM AM1/TIP3P calculations and the gas phase free energy profile is plotted. For selected structures, the free energy of solvation calculated by Monte Carlo simulation is also plotted in the same diagram. Sum of these two curves are shown in Fig. 6 which give the free energy profile in aqueous solution.

It can be seen that the activation energy (E_a) of the reaction is higher in gas phase than in aqueous phase. This is due to the charge delocalization in TS which stabilizes the TS in aqueous phase more than reactants and causes a decrease in E_a which in turn increases the rate of reaction as expected. The computed free energy of activation in the water media is 22.89 kcal/mol which is close to the experimental value 21.00 kcal/mol (Table 2).

Hydrogen bond analyses were performed on 990 configurations (one saved in every 10 K configurations). For this purpose a hydrogen bond is defined with a minimum interaction of 2.25 kcal/mol and a H…Y distance of less than 2.5Å. The solute-solvent energy pair distributions record the average number of solvent molecules that interact with the solute, and the associated energy. The results for the TS and reactants in the water media are shown in Fig. 7. Hydrogen bonding is reflected in the left-most region, with interaction energies of less attractive than -2.25 kcal/mol. The large peak near 0 kcal/mol results from the many distant solvent molecules in outer shells. It is observed from Fig. 7 that TS has lower energy bands compared to the reactants in water solution, arising from the water molecules forming stronger hydrogen bonds with TS. Integration of the bands yields 5.12 and 5.77 water molecules with an average strength -4.65 and -3.60 kcal/mol for the TS and reactants. Clearly, a

major source of the rate enhancement in the water media comes from increment stabilization of the TS compared to the reactants.
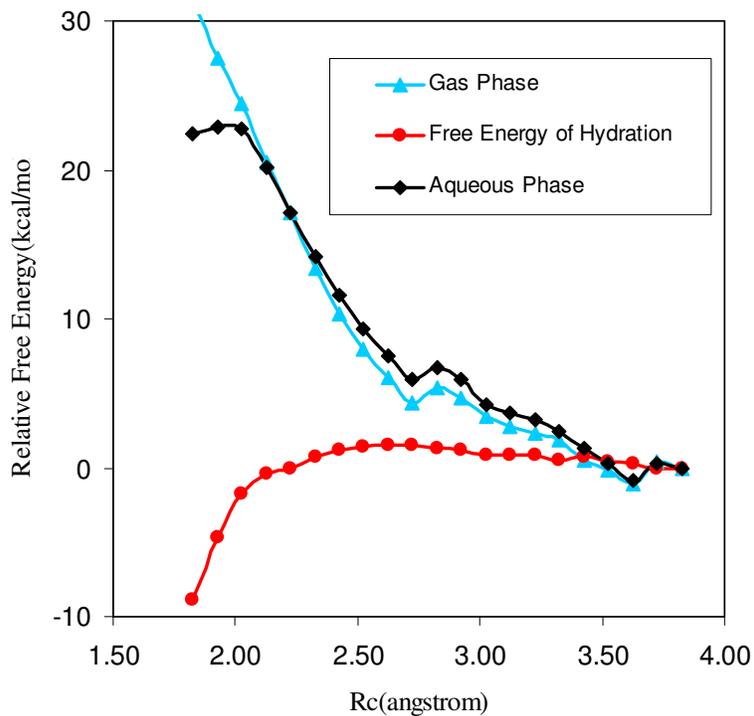

Figure 6. Free energy profile in gas phase and aqueous phase
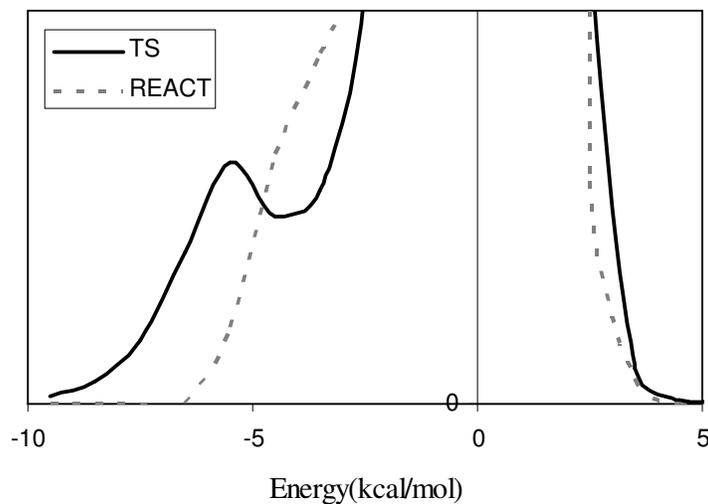
Figure 7. Solute-solvent energy pair distributions for the reaction of path A, Scheme 3 in water media

3.5.4. Optimization of water molecules in reaction media

In order to study the solvent effects from structural point of view, the optimizations were carried out in the present of the water molecules. The key geometrical parameter of TS and activation energy are shown in Scheme 6.

TS1
E_a (kcal/mol): 48.7
a)

TS4
43.14
b)
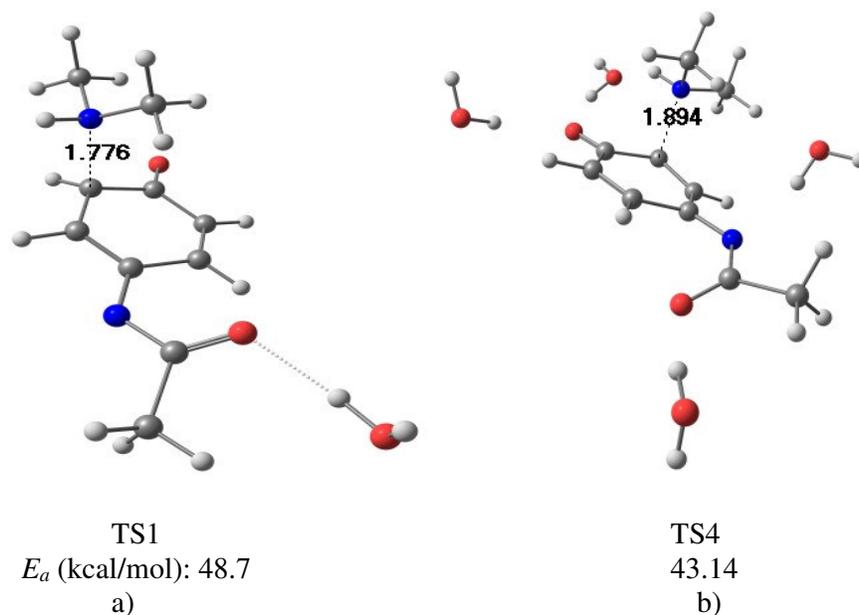
Scheme 6. Optimized structure of TS and activation energy of the reaction in presence of (a) one, (b) four water molecule(s).

Obtained results show that Rc at transition state shifts toward reactants and activation energy decrease by increasing the water molecules. The most important finding in the present study is that the Monte Carlo simulation confirms these results. There is a shift of 0.2 Å on the transition state toward the reactants which is in accordance with empirical expectations (See Fig. 6). In other words, the potential energy surface in aqueous phase is slower than gas phase in the mentioned reaction.

4. CONCLUSIONS

The results of this work show that acetaminophen is oxidized to *N*-acetyl-*p*-quinoneimine. The *N*-acetyl-*p*-quinoneimine is then attacked by dimethylamine to form amino-quinoneimine derivative as final product. In addition, the kinetics for the reaction of the electrogenerated *N*-acetyl-*p*-quinoneimine with dimethylamine is studied by cyclic voltammetry technique. The cyclic voltammograms were digitally simulated under *ECE* mechanism. The simulated cyclic voltammograms show good agreement with those obtained experimentally. Also, the theoretical calculations showed that: a) The product of reaction is only *N*-(3-dimethylamino-4-hydroxyphenyl)acetamide. b) Geometrical

parameters and charge calculations show that these reactions proceed through the 1,4-Michael addition mechanism and first step of mentioned reaction is rate determining step. c) This is a nice example of a bi-molecular reaction for which the TS is more polar than the reactants and therefore stabilized in solution TS in comparison with the reactants.

References

1. N. P. Vermeulen, J. G. Bessems and R. Van de Straat, *Drug Metab. Rev.,* 24 (1992) 367.
2. L. F. Prescott, *Paracetamol (Acetaminophen) a Critical Bibliographic Review*, Taylor & Francis Ltd., London, (1996) 285–351.
3. J. G. M. Bessems and N. P. E. Vermeulen, *Crit. Rev. Toxicol.*, 31 (2001) 55.
4. D. C. Dahlin and S. D. Nelson, *J. Med. Chem.,* 25 (1982) 885.
5. D.W. Potter and J. A. Hinson, *J. Biol. Chem.,* 262 (1987) 966.
6. A. R. Buckpitt, D. E. Rollins and J. R. Mitchell, *Biochem. Pharmacol.,* 28 (1979) 2941.
7. C. R. Fernando, I. C. Calder and K. N. Ham, *J. Med. Chem.,* 23 (1980) 1153.
8. E. Albano, M. Rundgren and P. J. Harvison, *Mol. Pharmacol.,* 28 (1985) 306.
9. D. W. Potter, D. W. Miller and J. A. Hinson, *Mol. Pharmacol.,* 29 (1986) 155.
10. E. Valero, R. Varón and F. Garcĺa-Carmon, *Arch. Biochem. Biophys.,* 416 (2003) 218.
11. E. Valero, P. Carrión, R. Varón and F. Garcĺa-Carmon, *Anal. Biochem.,* 318 (2003) 187.
12. D. D. Dahlin, G. T. Miwa, A. Lu and S. D. Nelson, *Proc. Natl. Acad. Sci.,* 81 (1984) 1327.
13. A. Albano, M. Rundgren, P. J. Harvison, S. D. Nelson and P. Moldeus, *Mol. Pharmacol.,* 28 (1985) 306.
14. S. S. Lee, J. T. Buters, T. Pineau, P. Fern_andez-Salguero and F. J. Gonz_alez, *J. Biol. Chem.,* 271 (1996) 12063.
15. J. A. Hinson, L. R. Pohl, T. J. Monks, J. R. Gillette and F. P. Guengerich, *Drug Metab. Dispos.*, 8 (1980) 289.
16. A. J. Forte, J. M. Wilson, J. T. Slattery and S. D. Nelson, *Drug Metab. Dispos.,* 12 (1984) 484.
17. W. Chen, L. L. Koenigs, S. J. Thompson, R. M. Meter, A. E. Rettie, W. F. Trager and S. D. Nelson, *Chem. Res. Toxicol.,* 11 (1998) 295.
18. D. J. Jollow, S. S. Thorgeirsson, W. Z. Potter, M. Hashimoto and J. R. Mitchell, *Pharmacolog.,* 12 (1974) 251.
19. M. Davis, N. G. Harrison, G. Ideo, B. Portmann, D. Labadarios and R. William, *Xenobiotica.,* 6 (1976) 249.
20. P. T. Kissinger, D. A. Roston, J. J. Van Benschoten, J. Y. Lewis and W. R. Heineman, *J. Chem. Educ.,* 60 (1983) 772.
21. D. J. Miner, J. R. Rice, R. M. Riggin and P. T. Kissinger, *Anal. Chem.,* 53 (1981) 2258.
22. K. Waterston, J. W. Wang, D. Bejan and N. J. Bunce, *J. Appl. Electrochem.,* 36 (2006) 227.
23. C. Wang, C. Li and F. Wang, *Microchimica Acta*, 155 (2006) 365.
24. G. Erdogdu and A. E. Karago*, Talanta,* 44 (1997) 2011.
25. Y. Z. Fang, D. Long and J. Ye, *Anal. Chim. Acta,* 342 (1997) 13.
26. R. M. de Carvalho, R. S. Freire1, S. Rath and L. T. Kubota, *J. Pharm. Biomed. Anal.,* 34 (2004) 871.
27. N. Wangfuengkanagul and O. Chailapakul, *J. Pharm. Biomed. Anal.,* 28 (2002) 841.

28. J. Tavakoli-Afshari and T. Liu, *Anal. Chim. Acta*, 443 (2001) 165.

29. R. Săndulescu, S. Mirel and R. Oprean, *J. Pharm. Biomed. Anal.,* 23 (2000) 77.

30. T. Pérez-Ruiz, C. Martínez-Lozano, V. Tomás and R. Galera, *J. Pharm. Biomed. Anal.,* 38 (2005) 87.

31. M. Boopathi, M. Won and Y. Shim, *Anal. Chim. Acta,* 512 (2004) 191.

32. M. Rudolph, J. *Electroanal. Chem.,* 529 (2002) 97. See: http://www.digielch.de/

33. M. J. Frisch, G. W. Trucks, H. B. Schlegel, G. E. Scuseria, M. A. Robb, J. R. Cheeseman, V. G. Zakrzewski, J. A. Montgomery, R. E. Stratmann, J. C. Burant, S. Dapprich, J. M. Millam, A. D. Daniels, K. N. Kudin, M. C. Strain, O. Farkas, J. Tomasi, V. Barone, M. Cossi, R. Cammi, B. Mennucci, C. Pomelli, C. Adamo, S. Clifford, J. Chterski, G. A. Petersson, P. Y. Ayala, Q. Morokuma, K. Cui, D. K. Malick, A. D. Rabuck, K. Raghavachari, J. B. Foresman, J. Ciolowski, J. V. Ortiz, B. B. Stefanov, G. Liu, A. Liashenko, P. Piskorz, I. Komaromi, R. Gomperts, J. L. Martin, D. J. Fox, T. Kieth, M. A. Al-Laham, C. Y. Peng, A. Nanayakkara, C. Gonzalez, M. Challacombe, P. M. W. Gills, B. Jonhson, W. Chen, M. W. Wong, J. L. Andres, M. Head-Gordon, E. S. Replogle and J. A. Pople, *Gaussian 98, Revision A.7*, Gaussian, Inc., Pittsburgh PA, 1998.

34. W. J. Hehre, L. Random, P. V. R. Schleger and J. A. Pople. *Ab Initio Molecular Orbital Theory*, Wiley, New York, 1986.

35. H. B. Schlegel, C. Peng, P. Y. Ayala and M. J. Frisch, *J. Comput. Chem.,* 17 (1996) 49.

36. M. J. Field, M. Albe, C. Bret, F. Proust-De Martin and A. Thomas, *J. Comput. Chem.,* 21 (2000) 1088.

37. W. L. Jorgensen, J. Chandrasekar, J. D. Madura, R. W. Impey and M. L. Klein, *J. Chem. Phys.,* 79 (1983) 926.

38. W. L. Jorgensen, D. S. Maxwell and J. Tirado-Rives, *J. Am. Chem. Soc.,* 118 (1996) 11225.

39. M. Haqghu, M. Irani and M. R. Gholami, *Prog. React. Kin. Mech.,* 32 (2007) 29.

40. B. A. Brookes, P. C. White, N. S. Lawrence and R. G. Compton, *J. Phys. Chem., B* 105 (2001) 6361.

41. T. J. Monks and D. C. Jones, *Curr. Drug Metab.,* 3 (2002) 425.